Chapter 13
Effect of K_2CO_3 Addition on CO_2 Gasification Characteristics and Ash Sintering Behaviour of a Chinese Lignite at Different Temperatures and Pressures as Examined Using a High-Pressure Thermogravimetric Analyser

Jianbo Li, Zhezi Zhang, Jian Hao, Jiguang Zhang, Mingming Zhu, and Dongke Zhang

Abstract The gasification characteristics and the morphology of the residue ash from pressurised K_2CO_3-catalysed gasification of a Chinese lignite in CO_2 was investigated using a High-Pressure Thermogravimetric Analyser operating at pressure of 2.0 or 3.5 MPa and temperature between 750 and 900 °C for at least 2 h, after being heated from room temperature at 10 °C/min. The K_2CO_3 addition was varied from 0 to 10% w/w. Gasification characteristics of the K_2CO_3-doped lignite was determined by analysing the weight loss and conversion rate as a function of time whereas the ash morphology was analysed by using SEM–EDS. Results showed that at 3.5 MPa the in-situ weight loss of the lignite increased as K_2CO_3 addition ratio increased, suggesting that K_2CO_3 addition promoted lignite gasification. The conversion rate of the lignite correspondingly increased from 61 to 92% as the temperature elevated to 750 °C. An increase in the final temperature to 900 °C significantly promoted lignite gasification when K_2CO_3 was less than 5%, however this was not obvious for lignite with 10% K_2CO_3 addition. This is because the conversion rate of the

J. Li (✉)
Key Laboratory of Low-Grade Energy Utilization Technologies and Systems, Ministry of Education of PRC, Chongqing University, 174 Shazheng Street, Shapingba District, Chongqing 400044, China
e-mail: jianbo.li@cqu.edu.cn

Z. Zhang · M. Zhu · D. Zhang
Centre for Energy (M473), The University of Western Australia, 35 Stirling Highway, Crawley, WA 6009, Australia

J. Zhang
Huadian Electric Power Research Institute Co. Ltd, No.10 Xiyuan 1st Road, Xihu District, Hangzhou City 310030, Zhejiang, China

J. Hao
State Key Laboratory of High-Efficiency Utilization of Coal and Green Chemical Engineering, Ningxia University, Yinchuan 750021, China

lignite with 10% K_2CO_3 addition had exceeded 90% before the final temperature of 900 °C was reached. Furthermore, as pressure decreased from 3.5 to 2.0 MPa, the lignite gasification rate slowed down, with or without K_2CO_3 addition. Conversion rate of the lignite decreased from 61 to 42% while the temperature initially elevated to 750 °C. SEM–EDS analysis revealed that sintering of the lignite ash was not observed at 750 °C, but became apparent at 1% K_2CO_3 addition. The degree of ash sintering further aggravated at 5 and 10% K_2CO_3 addition. As the temperature increased from 750 to 900 °C, the ashes of the raw lignite and 1% K_2CO_3 doped-lignite remained largely similar, whereas the sizes of the 10% K_2CO_3-doped lignite ash was increased and the particle surfaces became smooth, suggesting an enhanced sintering of the ash. The formation of K-aluminosilicate and Ca-aluminosilicate of low-melting points in the ash was responsible for possible deactivation of the doped catalyst K_2CO_3 and the observed ash behaviour.

13.1 Introduction

Clean coal technologies including integrated gasification combined cycle (IGCC) and pressurised fluidised bed combustor (PFBC) are regarded as the most viable alternatives for clean coal utilisation and have gained increased technological and scientific interests (Wall and Liu 2002; Jing and Wang 2013a; Ye and Agnew 1998). To increase the throughput of coal and promote reaction intensity of gasification, higher operating pressures and the use of catalytic additives have been applied (Wall and Liu 2002; Ye and Agnew 1998; Sharma and Takanohashi 2008; Zhang and Zhang 2015a; Fan and Yuan 2016). For instance, operating PFBC at 10–15 atm and IGCC at 15–25 atm have been reported in the literature (Wall and Liu 2002; Gupta 2005). Moreover, the use of catalytic additives not only promote gasification reaction at relatively low temperatures, but also shift the product gas to the desired direction (Akyurtlu and Akyurtlu 1995). However, the gasification characteristics of coal are affected by the operating procedures including pressure, temperature and catalyst addition. The ash residue might also lead to ash sintering, bed agglomeration and ash deposition on gas circuits and heat exchangers, further influencing the system stability (Jing and Wang 2011a, 2013a, b; Jing and Zhu 2016). Investigating the gasification characteristics and ash sintering behaviour during pressurised catalytic gasification at varying operating conditions are therefore essential.

Gasification characteristics of solid fuels including coal and biomass have been intensively investigated (Liang and Xie 2018; Liu and Guan 2018a, b; Zhao and Zhang 2018; Takematsu and Maude 1991; Irfan 2011; Nzihou and Stanmore 2013; Lee and Kim 1995). It is known that the gasification reactivity of coal is dependent on coal rank and char structure, the inherent inorganic matter, and operation conditions. Typically, low-rank coals have widely spread reactivity, while high-rank

coals have low reactivities. The gasification characteristics could be promoted by the inorganic mineral matter mainly alkali and alkali earth (Lee and Kim 1995). Thus, additives are used to promoted gasification and reform composition of the gas yield (Wu and Wang 2011; Zhang and Kudo 2013; Jaffri and Zhang 2008). Among the catalysts reported in the literature and used in industrial practices, potassium carbonate is believed to have superior catalytic properties, which not only promotes gasification reactivity, but also shifts the products to methane-rich or hydrogen-rich gases (Wang and Jiang 2009; Hattingh and Everson 2011). Moreover, the gasification characteristics are also dependent on temperature and pressure of the reactors (Wall and Liu 2002). As gasification temperature increases, the gasification kinetics are promoted, promoting gasification of coal or char. Likewise, pressure has been found to significantly influence the volatiles yield and coal swelling during devolatilisation, changing the structure and morphology of the char generated. At higher pressures, char combustion and gasification reaction rate would be enhanced as more char particles of high porosity are formed at higher pressures. However, comprehensive study during pressurized K$_2$CO$_3$-catalytic gasification of typical Chinese lignite is still required for better comprehension its gasification characteristics.

Sintering characteristics of the ash during gasification have also been widely studied (Bai and Li 2011; Chen and Dai 2012; Zhang and Zhang 2015b). It has been reported that sintering characteristics of the ash are dependent on the chemistry and mineral composition of the ash, atmosphere, temperature as well as pressure (Jing and Wang 2011a, b, 2013a, b; Jing and Zhu 2016; Zhang and Zhang 2015b; Li and Huang 2010). Jing and Wang (2011b) reported that the presence of acidic oxides such as SiO$_2$ and Al$_2$O$_3$ might increase ash sintering temperature yet the increase in Fe$_2$O$_3$, CaO, Na$_2$O, and K$_2$O decreased ash sintering temperature monotonously. In addition, the effect of MgO on the sintering temperature is not obvious when MgO is increased above a certain limit. Meanwhile, Fe in the ash during gasification would be in the form of Fe^{2+} and react with other oxides to form liquid phases (van Li and Huang 2010), promoting ash sintering between ash particles. Besides, FeO appears to react with CaO, SiO$_2$, and Al$_2$O$_3$ to produce the low-temperature eutectics (Dyk and Waanders 2007). As the catalyst K$_2$CO$_3$ are added into coal during gasification, a portion of potassium would be retained the ash, increasing the presence of K and the mineral interactions associated with K, thereby increasing the propensity of ash sintering (Erickson and Benson 1992; Kühn and Plogmann 1983; Bruno et al. 1986). Different gasification atmospheres such as CO$_2$ and steam atmosphere would also lead to varied mineral interaction and thus different ash sintering temperature (Lee and Kim 1995; Erickson and Benson 1992; Formella and Leonhardt 1986; Duchesne and Hall 2014). In addition, the sintering characteristics of the ash is also dependent on gasification temperature: an increase in gasification temperature might promote mineral interactions as well as the release of the alkali and alkali earth contents (Zhao et al. 2016). As for pressure, the increase in pressure would influence mineral transformation by affecting reactions between minerals and accelerates the formation of high-temperature minerals. However, supplemental study on the sintering characteristics of the ash during both pressurized and K$_2$CO$_3$-catalysed conditions are still essential.

This paper presents an investigation into the gasification characteristics and the ash sintering behaviour during K_2CO_3-catalysed gasification of lignite with varying pressures, temperatures, and K_2CO_3 addition ratios examined. The lignite with or without K_2CO_3 addition was gasified in a high pressure Thermogravimetric Analyser (HP-TGA) at varying pressure, and temperatures. The weight loss curve as a function of temperature was analysed and the morphology and chemistry of the obtained ash samples were analysed. It is expected that this paper would provide better comprehension on the effect of operating procedures and K_2CO_3 addition on gasification characteristics and ash sintering behaviour during pressurised K_2CO_3-catalysed gasification.

13.2 Experimental

13.2.1 Materials

A Chinese lignite, namely Wangjiata (WJT for short) lignite, was used during experimentation. The lignite was pulverised and sieved to particles less than 200 μm. Proximate and ultimate analysis of the lignite, chemistry of the ash prepared at 815 °C in air, and the ash fusion temperatures are shown in Table 13.1. Note that the volatile matter of WJT was 30.85% while its ash content was 26.5%. Moreover, the carbon content of the lignite was 75% and H was less than 4.10%. In terms of the ash chemistries, the WJT ash was rich in acidic oxides mainly SiO_2 (58.1%) and Al_2O_3 (12.1%), accounting for 60.2% of the total ash. Basic oxides such as CaO (11.5%) and Fe_2O_3 (6.3%) were also presented, and might contribute to ash sintering. As a consequence, the fusion temperatures of the ash were relatively low compared with other lignite or bituminous ash (Li and Zhu 2017).

K_2CO_3 was used as the catalyst for catalytic gasification. K_2CO_3 was analytical potassium carbonate with an impurity higher than 99.99%. During sample preparation, the lignite sample was firstly mixed with deionized water at a ratio of 10 ml (water)/1 mg (lignite) to form water-lignite slurry. K_2CO_3 with addition ratios of 1, 5 and 10 wt% (relative to lignite), respectively, was then dissolved into the water-lignite slurry. The mixture was then stirred by using a magnetic stirrer with a speed of 500r/min for 6 h. This was followed by drying in an oven at 60 °C to obtain the dried K_2CO_3-doped sample. These samples were denoted as WJT, WJT+1%K_2CO_3, WJT+5%K_2CO_3, and WJT+10%K_2CO_3 throughout this paper.

13.2.2 Experimental Setup

A high pressure Thermogravimetric Analyser (HP-TGA-150S, TA, US) as shown in Fig. 13.1 was used during experimentation. The HP-TGA was comprised of a

Table 13.1 Proximate and ultimate analysis of WJT lignite and its ash chemistry and fusion temperatures

	Proximate analysis (wt%)			Ultimate analysis (wt%)				
	A	V	FC	C	H	O	N	S
WJT	26.5	30.9	42.7	75.3	4.1	8.2	0.9	0.4

	Ash composition (wt%)							Fusion temperatures (°C)			
	SiO$_2$	Al$_2$O$_3$	CaO	Fe$_2$O$_3$	K$_2$O	Na$_2$O	SO$_3$	DT	ST	HT	FT
WJT	58.1	12.1	11.5	6.3	2.1	2.7	2.3	1130	1212	1260	1311

Fig. 13.1 Experimental setup of **a** the HP-TGA-150S system and **b** its main components
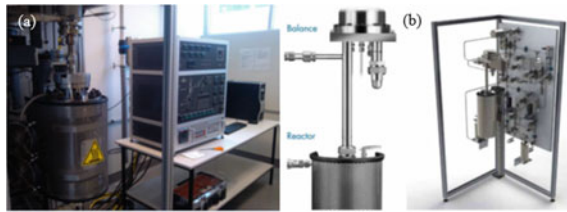
reactor, control system, and gas system. The reactor was made of stainless steel, which could be heated to 1100 °C and stand for 5.0 MPa. Moreover, five gas inlets were designed for input of various gases. The key components of the system are illustrated in Fig. 13.1b. A Rubotherm magnetic balance was used to measure the weight of the sample (and crucible), and the accuracy of the balance was $\pm 30 \mu g$.

During experimentation, the balance was firstly elevated above the reactor and ca. 0.2 g K_2CO_3-doped lignite was loaded into the crucible. The balance was then sent back to the reactor. For gasification at 2.0 MPa, pure CO_2 with a flow rate of 1L/min was used to elevate the pressure to 2.0 MPa. Whereas for gasification at 3.5 MPa, N_2 with a flow rate of 0.75 L/min was also provided at the same CO_2 flow rate. The reactor was then heated with a heating rate of 10 °C/min from ambient temperature to final temperatures of 750 to 900 °C, respectively. The experimentation maintained at the final temperatures for at least 2 h, and the weight of the sample (and crucible) was simultaneously recorded. Once the experimentation was finished, the reactor was cooled down to room temperature at N_2 atmosphere and the ash sample was afterwards collected.

13.2.3 Data Processing and Analysis

The in-situ weight loss curve as a function of time of each sample was corrected to eliminate the buoyancy effect. This correction included the correction of the magnet assembly, the sample holder, and the sample volume, i.e., Eq. 13.1,

$$Wt = W_0 + Wt_1 + Wt_2 + Wt_3 \tag{13.1}$$

where Wt the final weight of the lignite (g), W_0 the in-situ recorded sample weight (g), Wt_1, Wt_2, and Wt_3 the corrected weight (g) of the magnet assembly, sample holder, and sample volume, respectively.

Wt_1 was obtained based on the temperature, pressure and the corrected factor as shown in Eq. 13.2. P is the pressure of the system (bar), MW the mole weight of CO_2 or CO_2/N_2 mixture (g/mol), Z_1 the correction factor of the magnet assembly, and T_0 the set temperature of the assembly, 50 °C in this case.

$$Wt_1 = (2.29 \times P \times MW)/(Z_1 \times 83.144 \times (273.16 + T_0)) \tag{13.2}$$

The correction factor Z_1 was determined based on the properties of the mixtures, as shown in Eq. 13.3, where ψ the mole fraction of the gas in the mixture, P_{N2} the partial pressure of N_2 in the system (bar), ρ_{N2} and ρ_{CO2} are the densities of the pure N_2 and CO_2 (g/cc) determined based on the pressure and temperature of the gas.

$$Z_1 = Z_{N2} + Z_{CO2} = \psi_{N2} \times (P_{N2} \times 28)/(83.144 \times \rho_{N2} \times (273.16 + T_0))$$
$$+ \ \psi_{CO2} \times (P_{CO2} \times 44)/(83.144 \times \rho_{CO2} \times (273.16 + T_0)) \qquad (13.3)$$

Wt_2 was corrected based on Eq. 13.4 as below. Among Eq. 13.4, P is the pressure of the system (bar), MW the mole weight of the CO_2 or CO_2/N_2 mixture (g/mol), Z_2 the correction factor of the sample holder, and T the temperature as measured by the thermocouple (°C)

$$Wt_2 = (0.668 \times P \times MW)/(Z_2 \times 83.144 \times (273.16 + T)) \qquad (13.4)$$

The correction factor of the sample holder Z_2 was determined based on the properties of the gas mixtures, as shown in Eq. 13.5. ψ is the mole fraction of the gas in the mixture, P_{N2} the partial pressure of N_2 in the system (bar), ρ_{N2} and ρ_{CO2} the densities of the pure N_2 and CO_2 (g/cc) determined based on the pressure and temperature of the gas, and T the temperature as measured by the thermocouple (°C)

$$Z_2 = Z_{N_2} + Z_{CO_2} = \psi_{N2} \times \left(P_{N_2} \times 28\right)/\left(83.144 \times \rho_{N_2} \times (273.16 + T)\right)$$
$$+ \ \psi_{CO_2} \times \left(P_{CO_2} \times 44\right)/\left(83.144 \times \rho_{CO_2} \times (273.16 + T)\right) \qquad (13.5)$$

The sample weight after correction of magnet assembly and sample holder (Wt') was thus obtained as shown in Eq. 13.6, and the volume of the sample V_1 was obtained as Eq. 13.7

$$Wt' = W_0 + Wt_1 + Wt_2 \qquad (13.6)$$

$$V_1 = Wt'/2.2 \qquad (13.7)$$

Wt_3 was correction of sample volume based on Eq. 13.7, where V_1 the volume of the sample, P the pressure of the system (bar), MW the mole weight of CO_2 or CO_2/N_2 mixture (g/mol), Z_3 the correction factor of sample volume, the same as that of sample holder Z_2.

$$Wt_3 = (V_1 \times P \times MW)/(Z_3 \times 83.144 \times (273.16 + T)) \qquad (13.8)$$

Once the weight of the lignite was corrected, the conversion rate as a function of time was also obtained. The conversion rate (α) of the lignite was determined as the amount of weight loss relative to the overall weight loss after gasification (Eq. 13.9), where m_0 represents the initial sample weight, m_1 the final sample weight, and

m_i the sample weight during gasification at time i. Moreover, t_{50} during conversion, representing the time when 50% conversation rate was achieved, was also determined,

$$\alpha = (m_0 - m_i)/(m_0 - m_1) \tag{13.9}$$

13.2.4 SEM–EDS analysis

A TESCAN Vega 3 scanning electronic microscopy (SEM) coupled with X-ray energy dispersive spectroscopy (EDS) was used to analyse the morphological features and the chemistries of the obtained ashes. The chemistries of the ash particles were semi-quantitatively determined by the detector coupled in EDS.

13.3 Results and Discussion

13.3.1 Gasification Characteristics

13.3.1.1 Effect of K$_2$CO$_3$ Addition

Figure 13.2 illustrates the effect of K_2CO_3 addition on the weight loss and conversion rate of the K_2CO_3-doped lignite as a function of time during CO_2 gasification at 3.5 MPa in HP-TGA. The temperature profile during gasification was also recorded and are shown in Fig. 13.2. Based on the temperature profile as recorded, the weight loss as a function of time were divided into two periods. The first period was non-isothermal gasification during which temperature was increased from ambient temperature (<100 °C) to 750 °C. Note that the recorded temperature might be higher than 750 °C due to system response. The second period was the isothermal gasification period at 750 °C.
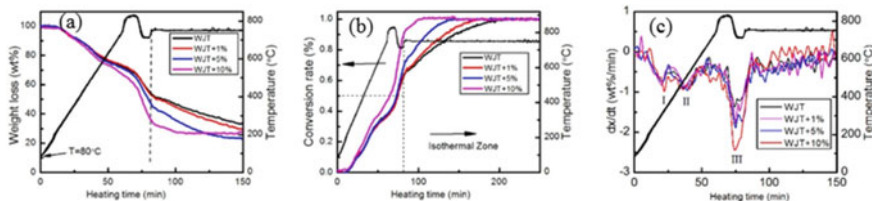

Fig. 13.2 Effect of K$_2$CO$_3$ addition on the **a** weight loss and **b** conversion rate of WJT during CO$_2$ gasification at 3.5 MPa and 750 °C

During non-isothermal gasification as shown in Fig. 13.2a, the weight of WJT decreased to 55 wt% as temperature increased to 750 °C. The sample weight further decreased slowly and reached to ca. 40 wt% after gasification at 750 °C for 150 min. This indicates that gasification of WJT without catalysts might be quite slow. Moreover, Gasification at this moment was believed to be incomplete as the ash content (Table 13.1) as determined ca. 26.5% was much less than the current of 40 wt%. As 1% K$_2$CO$_3$ was added into the lignite, the weight loss of WJT+1% K$_2$CO$_3$ was similar to that of WJT before the temperature reached 750 °C, which was however decreased faster at isothermal temperature of 750 °C and to ca. 30 wt% after gasification for 150 min. This indicated that the addition of 1% K$_2$CO$_3$ might not significantly promoted gasification at temperatures less than 750 °C, but would be apparent at 750 °C. As K$_2$CO$_3$ addition ratio further increased to 5% and 10%, the weight loss of the sample at the same time (and temperature) further increased, revealing that addition of 5 and 10% K$_2$CO$_3$ further promoted gasification. It is noted that the weight of WJT+10% K$_2$CO$_3$ decreased to less than 40 wt% while the temperature initially elevated to 750 °C. This enlightens that gasification was greatly promoted by the incorporating K$_2$CO$_3$. Moreover, the weight of WJT+10% K$_2$CO$_3$ at isothermal temperature of 750 °C was relatively stable after 20 min's gasification, while those with less K$_2$CO$_3$ required longer time. This again confirmed that addition of 10% K$_2$CO$_3$ promoted gasification of WJT.

Looking into the conversion rate of the lignite samples as shown in Fig. 13.2b, it is found that t_{50} of WJT, WJT+1% and WJT+5% were all at ca. 75 min. This illustrated that the addition of K$_2$CO$_3$, might not promoted gasification at lower temperatures. However, when the temperature was higher than 750 °C, the conversion rate was increased significantly. This implies that for gasification at temperatures lower than 750 °C, the effect of K$_2$CO$_3$ on gasification was not obvious when the addition ratio was in the range of 1–5%. However, at isothermal temperature 750 °C, the conversion rate became faster as K$_2$CO$_3$ addition increased from 0 to 5%, suggesting that the effect of K$_2$CO$_3$ on gasification at this range became significant. In comparison, t_{50} of WJT+10% was ca. 60 min, which was much earlier than those of lignites with less K$_2$CO$_3$ addition. This again indicates that addition of 10% K$_2$CO$_3$ promoted gasification even at lower temperatures.

13.3.1.2 Effect of Temperature

Figure 13.3 shows the effect of final temperature on the weight loss of WJT, WJT+1% K$_2$CO$_3$, and WJT+10% K$_2$CO$_3$ during CO$_2$ gasification at 3.5 MPa. It can be seen that for gasification of WJT (Fig. 13.3a), the sample weight decreased to 55 wt% as temperature elevated to 750 °C. The weight loss curves during heating stage was largely the same, confirming the repeatability of the experiments. During isothermal gasification, the sample weight at 850 and 900 °C decreased faster than that at 750 °C, indicating that the increase in temperature from 750 to 900 °C promoted gasification. Similar findings were also observed for lignite with 1% K$_2$CO$_3$ addition. However, when K$_2$CO$_3$ addition was increased to 10% as shown in Fig. 13.3c, the sample
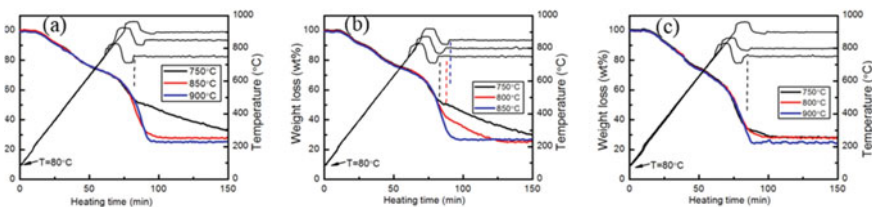
Fig. 13.3 Effect of Temperature on the weight loss of **a** WJT, **b** WJT+1% K_2CO_3, and **c** WJT+10% K_2CO_3 during CO_2 gasification at 3.5 MPa

weight decreased to less than 35 wt% during isothermal gasification, further proved that more K_2CO_3 would promote gasification. During isothermal gasification at 750, 800, or 900 °C, however, the differences in weight loss were not obvious. This is because gasification was nearly completed during heating stage, and the final temperature was thus insignificant for gasification.

13.3.1.3 Effect of Pressure

Figure 13.4 reveals the effect of pressure on the weight loss and conversion rate of WJT and WJT+10% K_2CO_3 as a function of time during CO_2 gasification at 750 °C. It is clear that at 2.0 MPa, the weight of WJT decreased to 70 wt% as temperature increased to 750 °C, and further decreased to 50 wt% after gasification for 350 min. This is much lower than that of WJT at 3.5 MPa of ca. 55% at 750 °C, and to 26 wt% after gasification (nearly completed) within the same time. These indicate that the increase in pressure promoted gasification of WJT. This was also applied for the weight loss of WJT+10% K_2CO_3 as illustrated in Fig. 13.4. The decrease in pressure promoted gasification of WJT+10% K_2CO_3. Moreover, the weight loss of WJT at 3.5 MPa was faster than that of WJT+10%K_2CO_3, suggesting that the effect of pressure on gasification might be superior to the effect of 10%K_2CO_3 addition.

It is also noted that t_{50} of these lignites decreased from 105 to 75, and 60 min as pressure increased to 3.5 MPa and K_2CO_3 addition to 10%, proving that the increase in pressure and pressure increased gasification of WJT. Moreover, the conversion
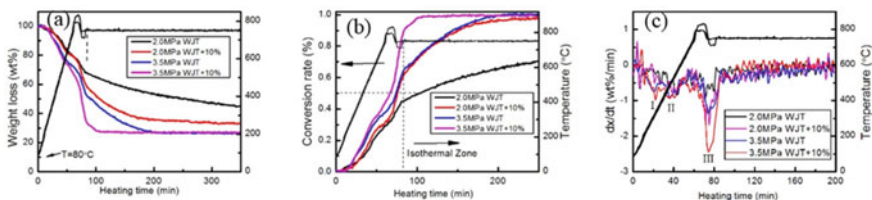

Fig. 13.4 Effect of pressure on the **a** weight loss and **b** conversion rate of WJT and WJT+10% K_2CO_3 during CO_2 gasification at 750 °C and pressures of 2.0 and 3.5 MPa

rate of WJT+10% K$_2$CO$_3$ at 2.0 MPa was less than that of WJT at 3.5 MPa when in non-isothermal stage, however its conversion rate was comparably to WJT at 3.5 MPa during isothermal gasification at 750 °C. This implies that the effect of 10% K$_2$CO$_3$ on gasification might be dependent on temperature. The catalytic effect of K$_2$CO$_3$ on gasification was low at lower temperatures, which however became significant at 750 °C. However, the effect of pressure on gasification, was significant during both non-isothermal and isothermal stages.

13.3.2   Ash Morphology

13.3.2.1   Effect of K$_2$CO$_3$

Figure 13.5 presents the morphological features and EDS analysis of the residue ashes of WJT with K$_2$CO$_3$ addition ratios of 0, 1, 5, and 10% during CO$_2$ gasification at 750 °C. It is clear that the sizes and shapes of the ash particles varied. The sizes of the ash particles ranged from sub microns to 200 μm as observed from SEM analysis. The shapes of these ash particles were irregular, and sintering between ash particles was seldom observed. This implies that most ash particles had relatively high melting-points and were thus not sintered. As 1% K$_2$CO$_3$ was added into the lignite, its ash particles (Fig. 13.5b) were also irregular in shape yet finer ash particles were less observed, implying that these finer particles might sinter together and therefore increase their sizes. As K$_2$CO$_3$ addition ratio further increased to 5% and 10%, the sizes of the ash particles were further increased as shown in Fig. 13.5c, d. Sintering between ash particles was observed, indicating that the addition of K$_2$CO$_3$ promoted ash sintering of the lignite ash at 750 °C.

EDS analysis on the ashes of WJT (Fig. 13.5a) reveals that the ash particles were heterogeneous in nature with varied contents of Si, Al, Ca, Fe, K, and Ca. As K$_2$CO$_3$ was added into the lignite, the contents of K in the ash increased as shown in Fig. 13.5b–d), suggesting that more K were presented in the ash, as expected due to K$_2$CO$_3$ addition. Looking into the ash chemistries of the sintered ashes, such as particles 2 and 1 in Fig. 13.5c and particles 1–5 in Fig. 13.5d, it was found that these particles were enriched in Si and K, and occasionally Ca, indicating the presence of K silicates, Ca-silicates and the eutectics between K-Si-Ca. The presence of these minerals or eutectics of low-melting points therefore promoted sintering of the ash particles.

13.3.2.2   Effect of Temperature

The morphological features of the ash of WJT, WJT+1% K$_2$CO$_3$, and WJT+10% K$_2$CO$_3$ during gasification at 3.5 MPa but different temperatures are presented in Figs. 13.6, 13.7 and 13.8. It is observable that the morphological features of WJT (Fig. 13.6) at 750, 800, 850, and 900 °C were largely the same, composing of the
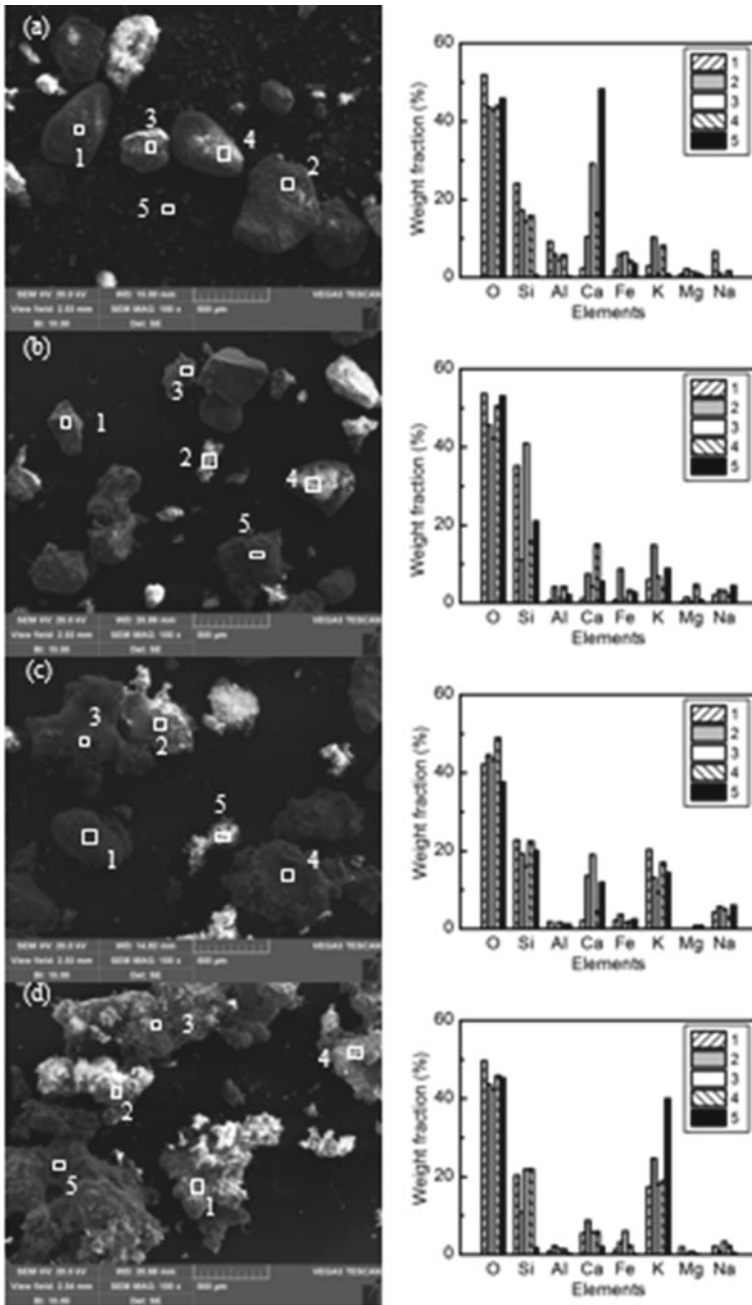
Fig. 13.5 Morphology of the obtained ashes during CO_2 gasification at 750 and 3.5 MPa of **a** WJT, **b** WJT+1% K_2CO_3, **c** WJT+5% K_2CO_3, and **d** WJT+10% K_2CO_3
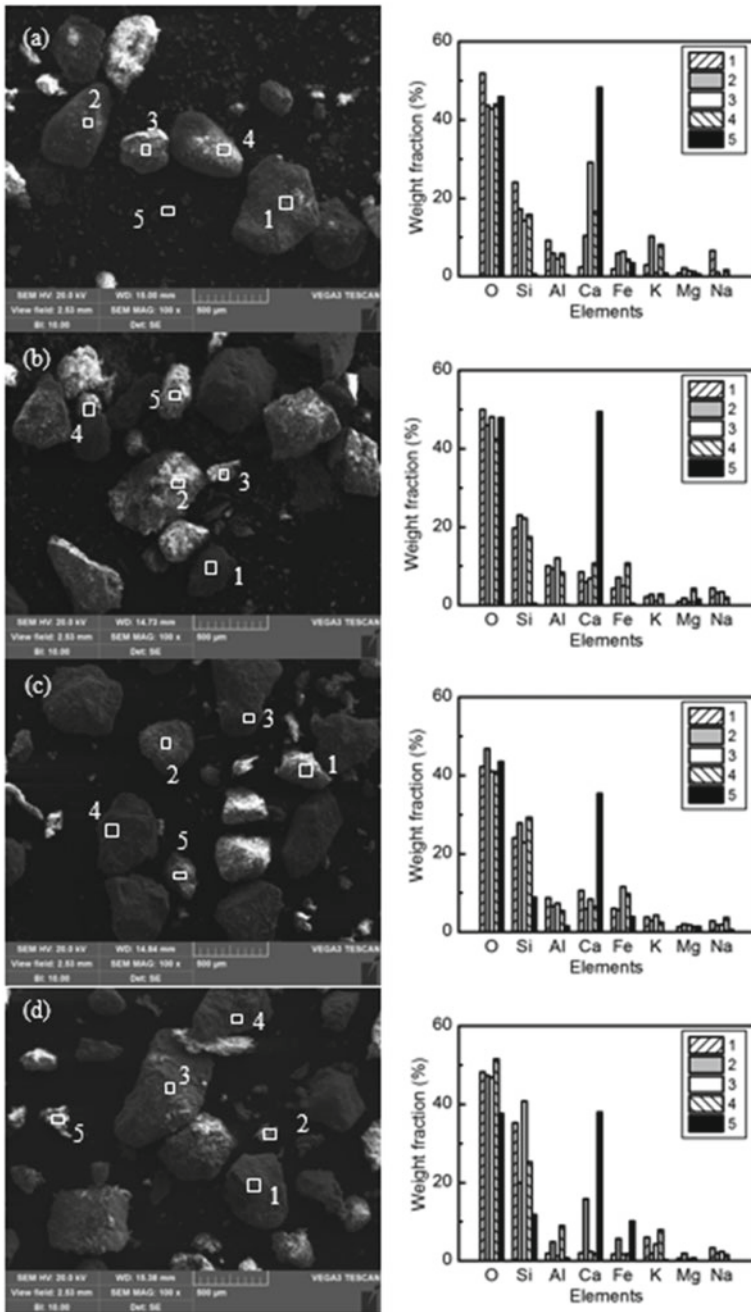
Fig. 13.6 Morphology of the obtained ashes during CO_2 gasification of WJT at 3.5 MPa, and temperatures of **a** 750 °C, **b** 800 °C, **c** 850 °C, and **d** 900 °C
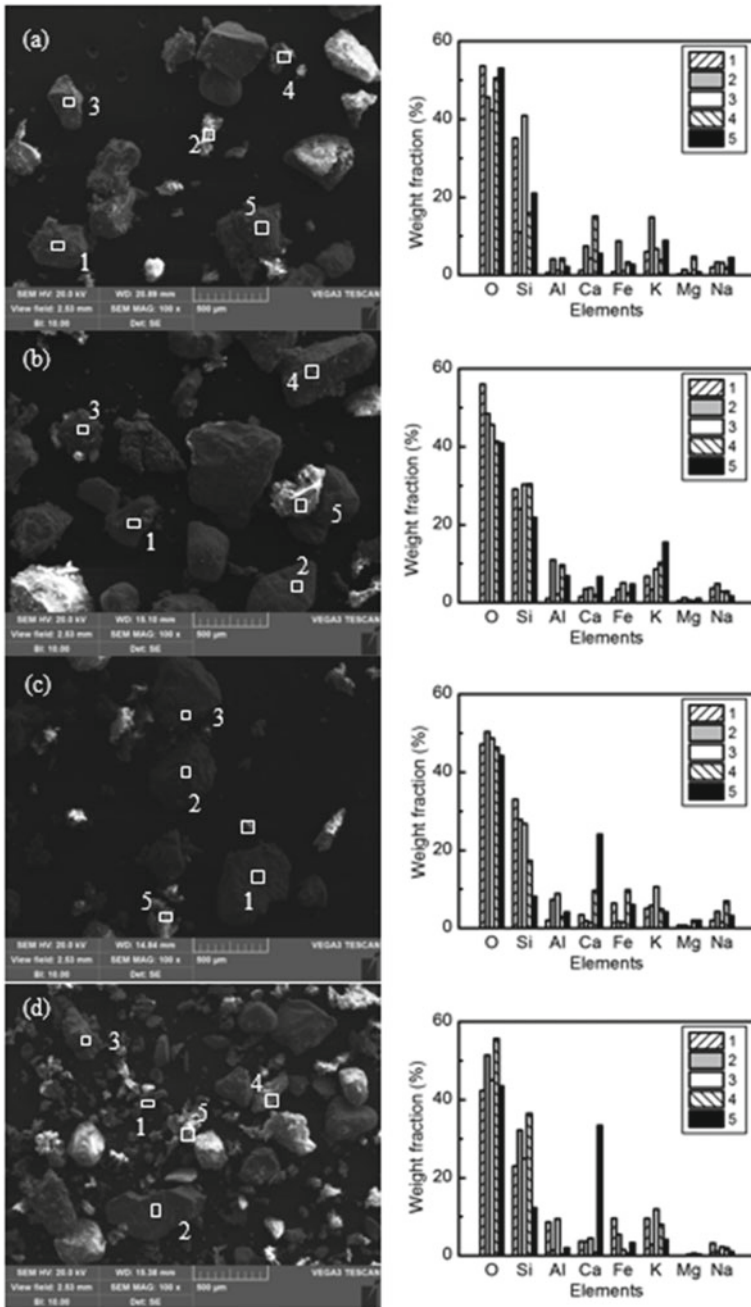
Fig. 13.7 Morphology of the obtained ashes during CO_2 gasification of WJT+1% K_2CO_3 at 3.5 MPa and temperatures of **a** 750 °C, **b** 800 °C, **c** 850 °C, and **d** 900 °C

Fig. 13.8 Morphology of the obtained ashes during CO₂ gasification of WJT+10% K₂CO₃ at 3.5 MPa and temperatures of **a** 750 °C, **b** 800 °C, **c** 850 °C, and **d** 900 °C
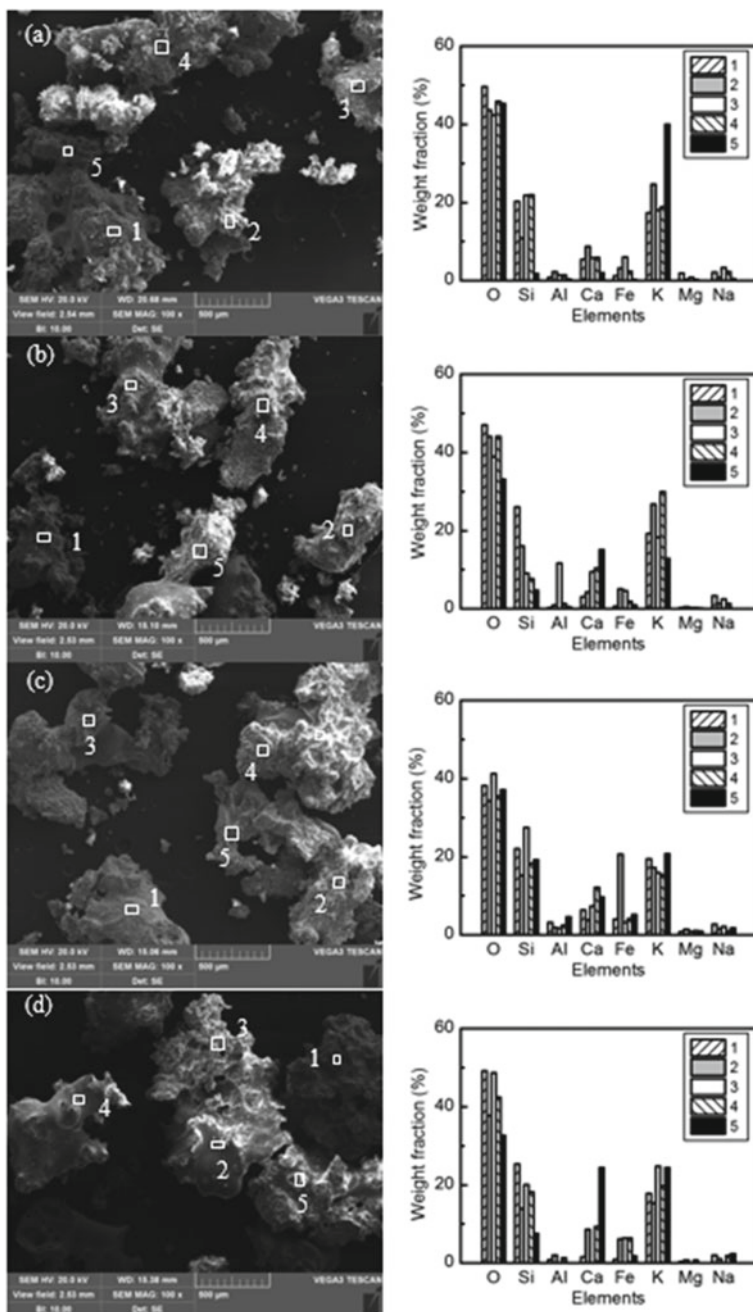
ash particles irregular in shape and varied in sizes. In particular, sintering between ash particles was not observed, indicating that the ash of WJT was resistant to the temperature change during gasification at 750–900 °C. Similarly, the ash morphologies of WJT+1% K_2CO_3 were quite the same, without significant differences being observed. Sintering between ash particles might occur as certain ash particles had sintered together (e.g., particle 3 in Fig. 13.7b). However, the remaining ash particles maintained its shapes and sizes during gasification. These imply that the ash of WJT+1% K_2CO_3 addition was less sintered and also resistant during gasification temperatures.

The morphological features of the ash of WJT+10% K_2CO_3 during gasification at 750–900 °C are illustrated in Fig. 13.8. It is obvious that sintering between ash particles had occurred at 750 °C. As temperature increased, the sizes of the ash particles tended to be increased and the surface of the ash particles became smooth at 900 °C. This indicates that the degree of ash sintering increased and more ashes had been melted at 900 °C. This also proves that ash sintering of WJT+10% K_2CO_3 was promoted as temperature increased from 750 to 900 °C.

EDS analysis on these ash particles showed that the ashes of WJT and WJT+1% K_2CO_3 ether rich in Si, Ca, Si/Al, or Si/Al/K (Particles in Figs. 13.6 and 13.7). As 10% K_2CO_3 was added into the lignite, its ash particles were composed of K, Si, and Ca, indicating that the eutectics between K, Si, and Ca were formed. The presence of low melting point eutectics thus increased sintering between ash particles.

13.3.2.3   Effect of Pressure

Figure 13.9 presents the morphological features of the ash of WJT and WJT+10% K_2CO_3 during CO_2 gasification at 2.0 MPa and temperatures of 750 °C and 850 °C. It can be seen that the ash of WJT at 750 °C was composed of ashes with different sizes and irregular in shape. Similar phenomena was also observed for the lignite ash obtained at 850 °C, consistent with the morphologies of the ash at 3.5 MPa. Likewise, the morphologies of the ashes of WJT+10%K_2CO_3 at 750 °C and 850 °C was also similar to those at 3.5 MPa. These suggest that the effect of pressure alone on the morphologies of the WJT and WJT+10%K_2CO_3 ashes might require further and comprehensive study.

13.4   Conclusions

The gasification characteristics and morphology of the residue ash during pressurised K_2CO_3-catalytic gasification of a lignite at CO_2 atmosphere but different temperatures, pressures and K_2CO_3 addition ratio was investigated a High-Pressure Thermogravimetric Analyser. Results showed that the addition of K_2CO_3 promoted gasification of the lignite. The effect of K_2CO_3 on gasification was not evident when K_2CO_3 addition ratio was 1%, but became significant when K_2CO_3 addition ratio
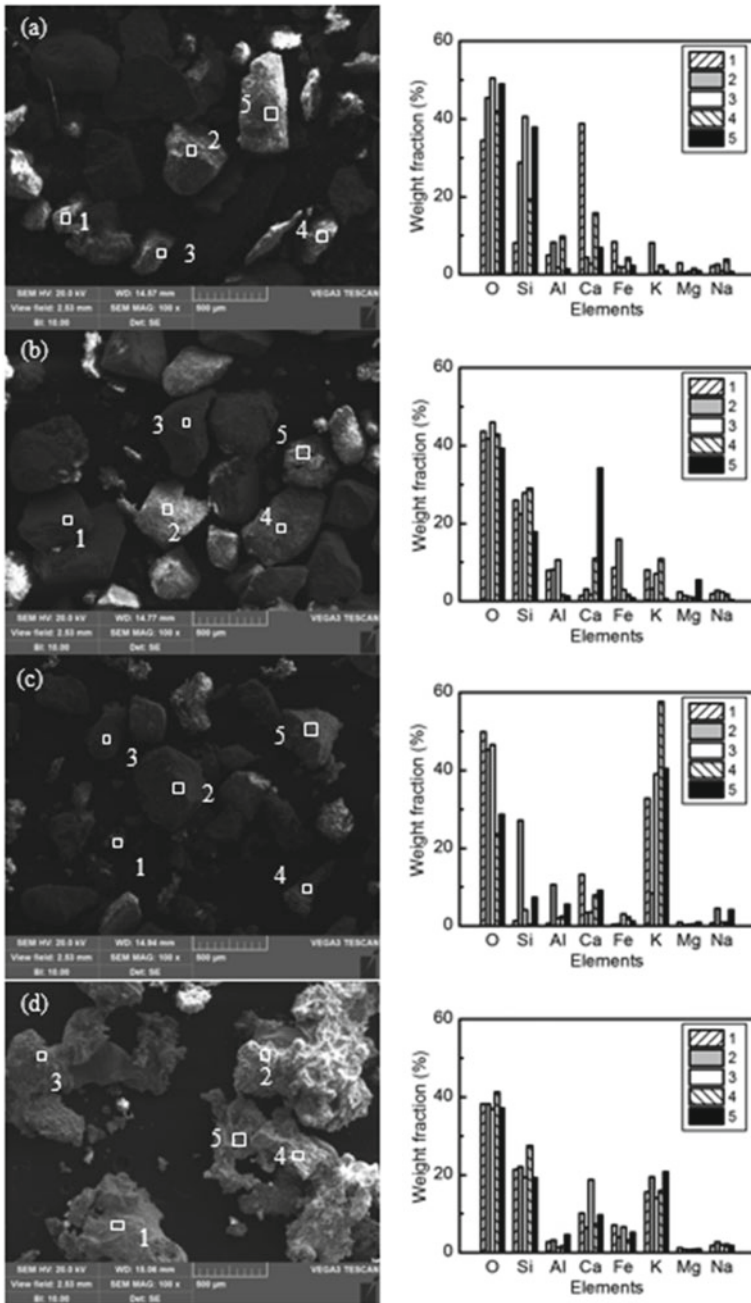
Fig. 13.9 Morphology of the ashes during CO₂ gasification at 2.0 MPa of **a** WJT at 750 °C **b** WJT at 850 °C, **c** WJT+10% K₂CO₃ at 750 °C, and **d** WJT+10% K₂CO₃ 850 °C

reached 10%. Furthermore, gasification of the lignite with 10% K_2CO_3 addition was almost completed even before the final temperature 750 °C was reached, bringing the conversion index t_{50} much earlier than those without K_2CO_3 addition. Moreover, both the increase in final temperature and pressure benefited gasification, regardless of K_2CO_3 addition. Yet, pressure played a significant role in gasification at all temperatures, while K_2CO_3 was mainly active at temperatures no less than 750 °C. SEM–EDS analysis on the obtained ashes revealed that sintering of the lignite ash was not observed at 750 °C, but was observed and the degree of ash sintering further aggravated as K_2CO_3 addition ratio increased to 10%. Likewise, as temperature and pressure increased, the sizes of the observed ash particles of the 10% K_2CO_3-doped lignite were increased and the surfaces of the ashes became smooth, incurring severe ash sintering. These observations were attributed to the presence of low-melting points K-aluminosilicate and Ca-aluminosilicate in the ash as identified.

References

Akyurtlu JF, Akyurtlu A (1995) Catalytic gasification of Pittsburgh coal char by potassium sulphate and ferrous sulphate mixtures. Fuel Process Technol 43(1):71–86

Bai J, Li W (2011) Effects of mineral matter and coal blending on gasification. Energy Fuels 25(3):1127–1131

Bruno G, Carvani L, Passoni G (1986) Correlation between potassium losses and mineral matter composition in catalytic coal steam gasification. Fuel 65(10):1473–1475

Chen J, Dai B (2012) XANES investigation on sulfur evolution during victorian brown coal char gasification in oxy-fuel combustion mode. Energy Fuels 26(8):4775–4782

Duchesne MA, Hall AD (2014) Fate of inorganic matter in entrained-flow slagging gasifiers: fuel characterization. Fuel Process Technol 118:208–217

Erickson T, Benson S (1992) Coal ash behavior in reducing environments. North Dakota University, Grand Forks, ND (United States). Energy and Environmental Research Center

Fan S, Yuan X (2016) Experimental and kinetic study of catalytic steam gasification of low rank coal with an environmentally friendly, inexpensive composite K_2CO_3–eggshell derived CaO catalyst. Fuel 165:397–404

Formella K, Leonhardt P (1986) Interaction of mineral matter in coal with potassium during gasification. Fuel 65(10):1470–1472

Gupta RP (2005) Research in Newcastle—past, present and future. Fuel 84(10):1176–1188

Hattingh BB, Everson RC (2011) Assessing the catalytic effect of coal ash constituents on the CO_2 gasification rate of high ash, South African Coal. Fuel Process Technol 92(10):2048–2054

Irfan MF (2011) Coal gasification in CO_2 atmosphere and its kinetics since 1948: a brief review. Energy 36(1):12–40

Jaffri G-e-R, Zhang J-Y (2008) Catalytic gasification characteristics of mixed black liquor and calcium catalyst in mixing (air/steam) atmosphere. J Fuel Chem Technol 36(4):406–414

Jing N, Wang Q (2011a) Effect of different reaction atmospheres on the sintering temperature of Jincheng coal ash under pressurized conditions. Fuel 90(8):2645–2651

Jing N, Wang Q (2011b) Effect of chemical composition on sintering behavior of Jingcheng coal ash under gasification atmosphere. Chem Eng Commun 199(2):189–202

Jing N, Wang Q (2013a) Effect of temperature and pressure on the mineralogical and fusion characteristics of Jincheng coal ash in simulated combustion and gasification environments. Fuel 104:647–655

Jing N, Wang Q (2013b) The sintering behavior of coal ash under pressurized conditions. Fuel 103:87–93

Jing N, Zhu M (2016) Effect of ash preparation method on the sintering characteristics of ashes from combustion of coal and biomass blends. Fuel 186:830–837

Kühn L, Plogmann H (1983) Reaction of catalysts with mineral matter during coal gasification. Fuel 62(2):205–208

Lee WJ, Kim SD (1995) Catalytic activity of alkali and transition metal salt mixtures for steam-char gasification. Fuel 74(9):1387–1393

Li F, Huang J (2010) Formation mechanism of slag during fluid-bed gasification of lignite. Energy Fuels 25(1):273–280

Li J, Zhu M (2017) Effect of coal blending and ashing temperature on ash sintering and fusion characteristics during combustion of Zhundong lignite. Fuel 195(Supplement C):131–142

Liang D, Xie Q (2014) Catalytic effect of alkali and alkaline earth metals in different occurrence modes in Zhundong coals. Asia-Pacific J Chem Eng 13(3):e2190

Liu Y, Guan Y-J (2018a) Gasification reactivity and morphology of coal chars formed in N₂ and CO₂ atmospheres. Chem Pap 7(8):2045–2054

Liu Y, Guan Y (2018b) CO₂ gasification performance and alkali/alkaline earth metals catalytic mechanism of Zhundong coal char. Korean J Chem Eng 35(4):859–866

Nzihou A, Stanmore B (2013) A review of catalysts for the gasification of biomass char, with some reference to coal. Energy 58:305–317

Sharma A, Takanohashi T (2008) Effect of catalyst addition on gasification reactivity of HyperCoal and coal with steam at 775–700°C. Fuel 87(12):2686–2690

Takematsu T, Maude C (1991) Coal gasification for igcc power generation. IEACR/37. IEA Coal Research, London

van Dyk JC, Waanders FB (2007) Manipulation of gasification coal feed in order to increase the ash fusion temperature of the coal enabling the gasifiers to operate at higher temperatures. Fuel 86(17–18):2728–2735

Wall TF, Liu GS (2002) The effects of pressure on coal reactions during pulverised coal combustion and gasification. Prog Energy Combust Sci 28(5):405–433

Wang J, Jiang M (2009) Steam gasification of coal char catalyzed by K₂CO₃ for enhanced production of hydrogen without formation of methane. Fuel 88(9):1572–1579

Wu Y, Wang J (2011) Potassium-catalyzed steam gasification of petroleum coke for H2 production: reactivity, selectivity and gas release. Fuel Process Technol 92(3):523–530

Ye DP, Agnew JB (1998) Gasification of a South Australian low-rank coal with carbon dioxide and steam: kinetics and reactivity studies. Fuel 77(11):1209–1219

Zhang L-X, Kudo S (2013) Catalytic effects of Na and Ca from inexpensive materials on in-situ steam gasification of char from rapid pyrolysis of low rank coal in a drop-tube reactor. Fuel Process Technol 113:1–7

Zhang J, Zhang L (2015a) Effect of bauxite additives on ash sintering characteristics during the K₂CO₃-catalyzed steam gasification of lignite. RSC Adv 5(9):6720–6727

Zhang J-G, Zhang L (2015b) Ash Sintering behavior of lignite in catalyzed steam gasification with kaolin as additive. Energy Technol 3(6):556–562

Zhao Y, Zhang W (2018) Kinetic characteristics of in-situ char-steam gasification following pyrolysis of a demineralized coal. Int J Hydrogen Energy 43(24):10991–11001

Zhao Y, Feng D, Zhang Y, Huang Y, Sun S (2016) Effect of pyrolysis temperature on char structure and chemical speciation of alkali and alkaline earth metallic species in biochar. Fuel Process Technol 141(Part 1):54–60